Supplementary Information

High-Performance Optoelectronics Enabled by Solution-Based Sintering of Perovskite Nanocrystals

Karthika Vijayan[1,2,3], Yu-Xiang Chen[3,4,5], Pradyumna Kumar Chand[1,2,3,6], Ting-Chun Huang[3], Ya-Ping Hsieh[3], and Mario Hofmann[1]*

Affiliation

1. Department of Physics, National Taiwan University, Taipei, 10617, Taiwan
2. Nanoscience and Technology Program, Taiwan International Graduate Program, Academia Sinica, Taipei, 105210, Taiwan
3. Institute of Atomic and Molecular Sciences, Academia Sinica, Taipei, 10617, Taiwan
4. Molecular Science and Technology Program, Taiwan International Graduate Program, Academia Sinica, Taipei, 105210, Taiwan
5. International Graduate Program of Molecular Science and Technology, National Taiwan University, Taipei 10617, Taiwan
6. Department of Chemistry, National Taiwan University, Taipei, 10617, Taiwan

*mario@phys.ntu.edu.tw

Materials and Methods

Material used

Cs_2CO_3 (Alfa Aesar, 99%), $PbBr_2$ (Alfa Aesar, 99.998%), Octadecene (ODE, TCI, 90%), *N*, *N* Dimethylformamide (DMF, Fisher), Oleic acid ($CH_3(CH_2)_7CH{=}CH(CH_2)_7COOH$, 88%, Showa), Hexanoic acid ($CH_3CH_2CH_2CH_2CH_2COOH$, Showa, 98.0%), Octylamine ($CH_3CH_2CH_2CH_2CH_2CH_2CH_2CH_2NH_2$, Alfa Aesar, 99%), Dodecyl amine ($CH_3CH_2CH_2CH_2CH_2CH_2CH_2CH_2CH_2CH_2CH_2CH_2NH_2$, Alfa Aesar, 97%), and Toluene (Mallinckrodt ultimAR, 99.8%) were purchased and used without further purification.

Nanocube Synthesis

$CsPbBr_3$ nanocubes were synthesized following the recipe of Shibin Sun et al.[1] which uses a reprecipitation process at room temperature. Cesium oleate is initially prepared by mixing 0.814g of Cesium carbonate and 10mL octadecene, into which 2.5mL oleic acid was added and dried at 120°C, heated to 150°C under N_2 atmosphere. For nanocube synthesis, 0.1mmol $PbBr_2$ was added to 2mL DMF. 1.55mmol of Oleic acid and 0.0866mmol dodecylamine were added later. After complete solubilization of $PbBr_2$, the previously prepared Cs-oleate (0.1mL) is added. 0.05mL of this hybrid solution was added to 2mL of toluene. This solution was centrifuged at 4000 rpm for 15mins and then ethanol washed and desiccator dried.

Mechano-coalesced flake synthesis

The above synthesized nanocubes were dispersed in Toluene (desired solvent) depending on the required concentrations ranging from 0.5mM to 4.5mM. Mechano-coalescent, dropcasted,

and spin-coated[2, 3] samples were prepared of similar solution concentrations. Different molar solutions of $CsPbBr_3$ perovskite nanocrystals (PNCs) dispersed in Toluene were spin-coated on different substrates (Si/SiO_2, Sapphire, FTO, and copper foil) at 3000rpm for 40s and baked at 60°C for 30 minutes.

For mechano-coalesced assembly, we used two different immiscible solvents (water and Toluene) that have different densities. Similarly, different substrates like glass, Si/SiO_2, sapphire, FTO, and copper foil were used to harvest the samples from the liquid-liquid interface. $CsPbBr_3$ nanocubes dispersed in Toluene were introduced into water at a rate of 100-330 µl/min. The mechanical force was provided through a rotator, which is in the range of 60-120rpm. Then, samples were harvested from the interface at different time intervals of rotation and were dried at 70 °C for 30-36 hours. We tried optimizing parameters by attempting with different concentrations of sample, different rpms, varied approach velocity, intermittently applying mechanical force, and avoiding chances of partial coalescence[4] as these parameters can lead to thickness in the resultant flakes obtained. The thinnest and largest flakes were obtained at a dispense rate of 300µl/min, at 100rpm where the substrate is 6mins O_2 etched Si/SiO_2 and dried for 32 hours at 70 °C in ambient conditions.

Characterization

The Ultra-high-resolution field emission scanning electron microscope (SEM) and energy dispersed spectroscopy (EDS) data were collected using JEOL JSM-7800F PrimeSEM at an electron energy of 10kV. Transmission electron microscopy (TEM) and SAED used 200kV field-

emission gun transmission electron microscope (FEI Tecnai G2 F20). Fourier transform infrared spectroscopy (FTIR) was carried out in a Horiba FT 720 spectrophotometer.

Optical micrographs were taken using Olympus BX53 with a CCD camera attached to it. Photoluminescence (PL), and temperature-dependent photoluminescence (TDPL) was performed using a custom-built PL measurement system equipped with a 405nm laser. Time-resolved photoluminescence (TRPL) measurements were obtained using NANOBASE XPER RF Raman system (NBOS-220012).

Electrochemical measurements like Cyclic Voltammetry (CV) and Electrochemical Impedance Spectroscopy (EIS)[23] were performed using a three-electrode system in conjunction with a CHI 660E electrochemical workstation. A platinum wire with a diameter of 3mm was used as a counter electrode, while an Ag wire with a diameter of 0.5mm coated with AgCl served as a quasi-reference electrode. The working electrodes were mechano-coalesced PNCs on FTO substrate. 0.1M Tetrabutylammonium hexafluorophosphate (NBu_4PF_6) in Acetonitrile was used as supporting electrolyte. CV data were measured from −1.6 to 1.6 V with a scan rate of 50 mV/s. EIS spectra were collected using the same experimental setup at a perturbation voltage amplitude of 1 V, within the frequency range from 0.1 Hz to 1 MHz. The parameters were calculated by fitting the Nyquist plot with an equivalent circuit.

Current-voltage measurements were carried out by depositing Au electrodes using e-beam evaporation with a stainless-steel shadow mask. During deposition, the temperature was monitored and kept under 55°C. A bias voltage of -1V to +1V was applied, and photoresponse was measured at a bias voltage of 9.5V under 405nm laser illumination.

FTIR Characterization

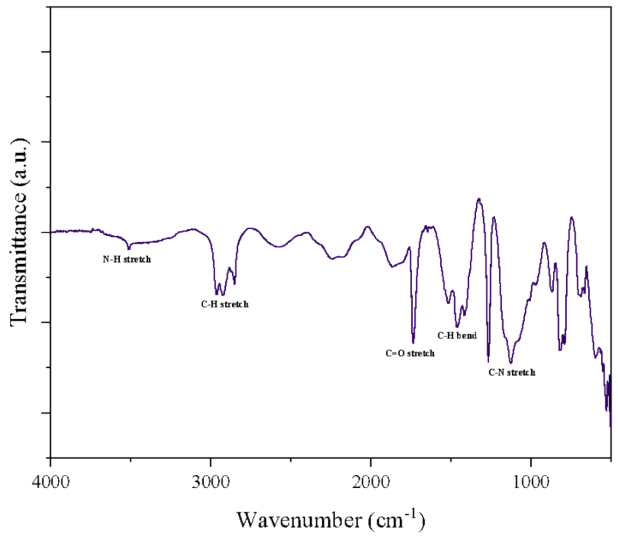

Fig S1. FTIR spectra of mechano-coalesced flakes with amine, carbonyl and alkane groups

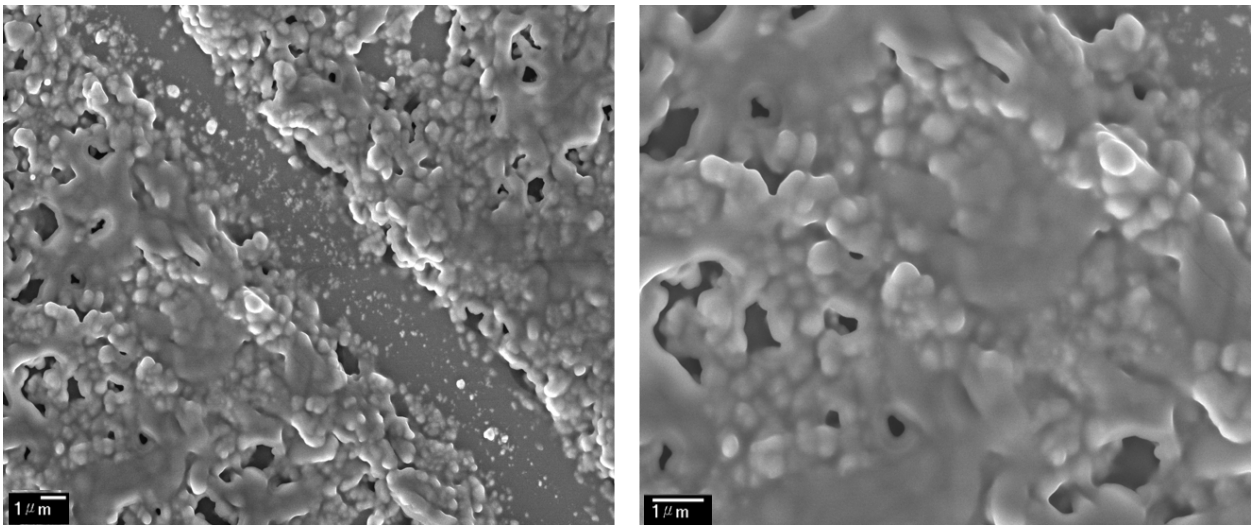

SEM characterizations

Fig. S2. SEM images of thick flakes obtained under high rpm

TEM characterization

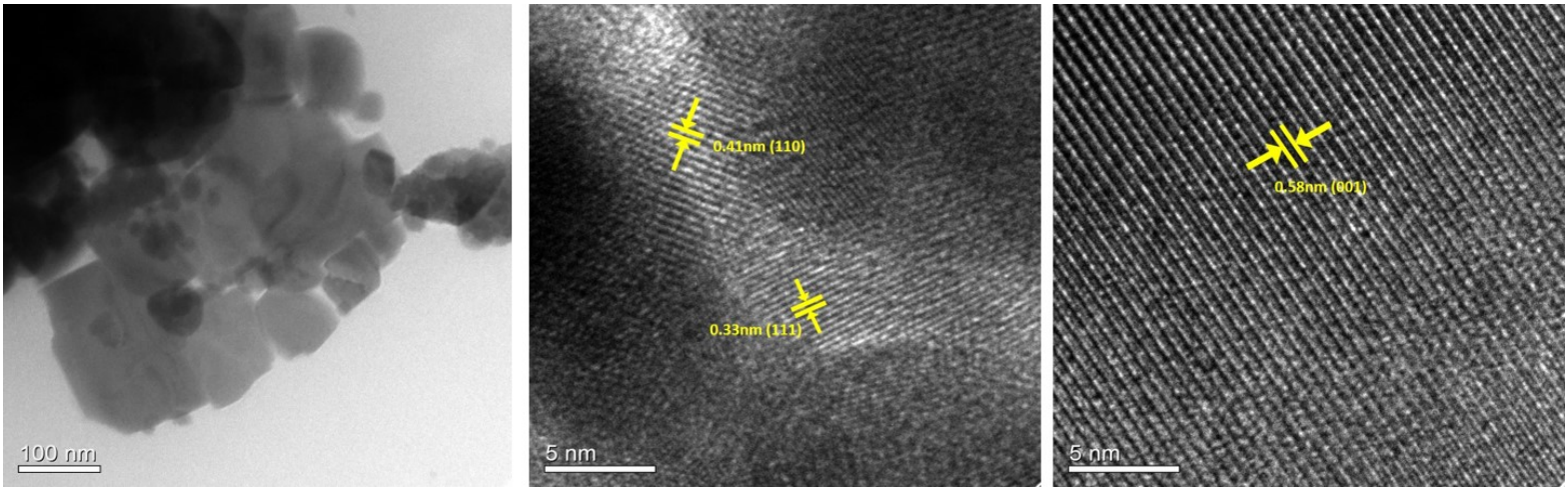

Fig.S3. TEM image of Flakes (without false coloration) and HRTEM images of mechanocoalesced flakes.

Temperature-dependent photoluminescence (TDPL)

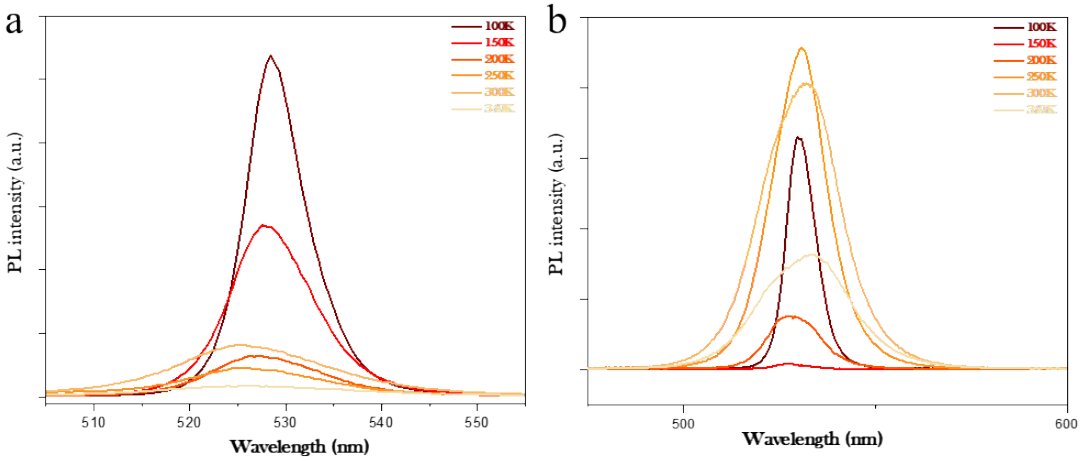

Fig. S4. TDPL of (a) Mechano-coalesced and (b) Dropcasted samples

Table S1. Quantum yield from Time-resolved photoluminescence (TRPL)

	A_1	τ_1 (ns)	A_2	τ_2 (ns)	η
Mechano-coalesced	671.1	1.532 ± 0.033	237.6	8.000 ± 0.618	73.85%
Dropcasted	63.52	2.000 (fixed at bound)	702.8	9.712 ± 0.308	8.28%

	Confidence interval: $\boldsymbol{\tau_1}$	Confidence interval: $\boldsymbol{\tau_2}$
Mechano-coalesced	1.532 (1.499, 1.565)	8 (7.382, 8.618)
Dropcasted	2.00 (fixed at bound)	9.712 (9.405, 10.02)

The amplitude weighted fractional contribution, η is determined using the formula,

$$\eta = \frac{A_1}{(A_1 + A_2)}$$

where A_1 is non-radiative recombination rate coefficient, and A_2 is radiative recombination rate coefficient. The yield of individual nanocubes is comparable to previous reports[5, 6].

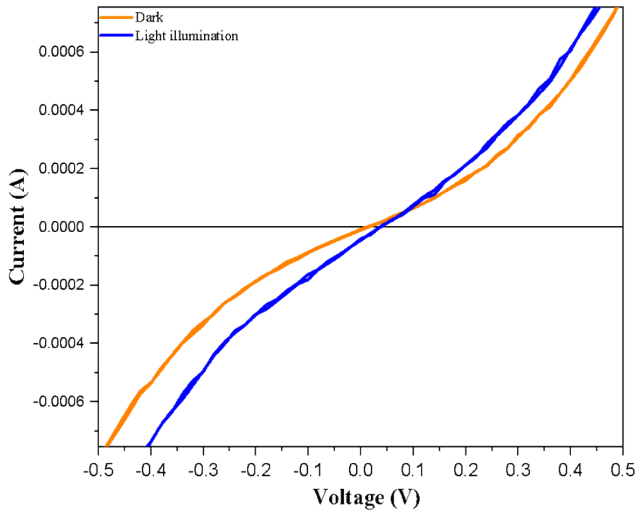

Current-Voltage measurements

Fig. S5. Current-voltage curves of mechano-coalesced perovskite flakes under light illumination and dark conditions

Table S2. Comparison table of previously reported values of detectivity

Material	**Wavelength(nm)**	**Detectivity (Jones)**	**Reference**
Our work	405	$1.149*10^{13}$	
$CsPbBr_3$	550	$3.6*10^{12}$	7
$CsPbBr_3$ Single crystal	450	$1.8*10^{11}$	8
$CsPbBr_3$ thin film	442	$6.1*10^{11}$	9
Solution-processed $CsPbBr_3$	532	$1.68*10^{9}$	10

Inverse temperature crystallized $CsPbBr_3$	550	$6.26*10^{10}$	11
$CsPb_2Br_5$ microwires	405	$6.07*10^{10}$	12
$CsPbBr_3$ nanowires	473	$1*10^{13}$	13
$CsPbBr_3$ thin film	405	$9*10^{12}$	14
$CsPbBr_3$ nanocrystals	405	$2.84*10^{9}$	15
$CsPbBr_3$ microcrystals	473	$4.8*10^{12}$	16
$MAPbBr_3$	532	$1*10^{12}$	17
α- $CsPbBr_3$	640	$1.8*10^{12}$	18
$CsPbBr_3$/$CsPb_2Br_5$ dual-phase composite	405	$4.7*10^{9}$	19
Single crystal $MAPbI_3$	660	$2.5*10^{11}$	20
$MAPbI_3$ on rocksalt	520	$6.5*10^{13}$	21
(PVP)-$MAPbI_3$	550	$2.23*10^{11}$	22
(PVP)-$MAPbI_3$	700	$1.01*10^{11}$	22

Table S3. Bias Conditions Summary

Condition	Bias Voltage (V)	Measurement Mode
Dark I-V	-1V to +1V	Swept voltage
Illuminated I-V	-1V to +1V	Swept voltage
Photoresponse (on-off switching)	9.5V	Pulsed illumination

Experimental Setup

Figure S6. Arrangement of the experimental setup

Table S4. Alternate solvent systems attempted instead of Toluene- water system

Main Phase	**Sub phase**	**Resulting morphology**
Toluene	Ethanol	Doesn't work; no flakes
	Methanol	No assembly, bigger individual rod structures
	IPA	Doesn't work; cubes fused forming optically inactive thick dark aggregates
Xylene	Water	Doesn't work; cubes dispersed into water with no flake formation
Hexane	Water	Hexane evaporated quickly leaving no residues
	Acetic acid	Doesn't work; no flakes
Anisole	Water	Doesn't work; no residues

References

(1) Sun, S.; Yuan, D.; Xu, Y.; Wang, A.; Deng, Z. Ligand-mediated synthesis of shape-controlled cesium lead halide perovskite nanocrystals via reprecipitation process at room temperature. *ACS nano* **2016**, *10* (3), 3648-3657.

(2) Zhang, B.; Chen, C.; Chen, X. High-Efficiency CsPbBr3 Light-Emitting Diodes using One-Step Spin-Coating In Situ Dynamic Thermal Crystallization. *Micromachines* **2023**, *14* (6), 1104.

(3) Li, B.; Li, X.; Li, X.; Liu, H.; Li, Z.; Xiang, G.; Liu, Y.; Zhou, T.; Fang, X.; Zhang, Z. A simple method to improve the performance of perovskite light-emitting diodes via layer-by-layer spin-coating CsPbBr 3 quantum dots. *RSC advances* **2018**, *8* (48), 27201-27206.

(4) Torza, S.; Mason, S. Coalescence of two immiscible liquid drops. *Science* **1969**, *163* (3869), 813-814.

(5) Zeng, F.-l.; Yang, M.; Qin, J.-l.; Teng, F.; Wang, Y.-q.; Chen, G.-x.; Wang, D.-w.; Peng, H.-s. Ultrastable luminescent organic–inorganic perovskite quantum dots via surface engineering: Coordination of methylammonium bromide and covalent silica encapsulation. *ACS Applied Materials & Interfaces* **2018**, *10* (49), 42837-42843.

(6) Liu, K.-K.; Liu, Q.; Yang, D.-W.; Liang, Y.-C.; Sui, L.-Z.; Wei, J.-Y.; Xue, G.-W.; Zhao, W.-B.; Wu, X.-Y.; Dong, L. Water-induced MAPbBr3@ PbBr (OH) with enhanced luminescence and stability. *Light: Science & Applications* **2020**, *9* (1), 44.

(7) Tran, P.-N.; Tran, B.-D.; Nguyen, D.-C.; Nguyen, T.-L.; Tran, V.-D.; Duong, T.-T. A Facile Centrifuge Coating Method for High-Performance CsPbBr3 Compact and Crack-Free Nanocrystal Thin Film Photodetector. *Crystals* **2022**, *12* (5), 587.

(8) Ding, J.; Du, S.; Zuo, Z.; Zhao, Y.; Cui, H.; Zhan, X. High detectivity and rapid response in perovskite CsPbBr3 single-crystal photodetector. *The Journal of Physical Chemistry C* **2017**, *121* (9), 4917-4923.

(9) Li, X.; Yu, D.; Cao, F.; Gu, Y.; Wei, Y.; Wu, Y.; Song, J.; Zeng, H. Healing all-inorganic perovskite films via recyclable dissolution–recyrstallization for compact and smooth carrier channels of optoelectronic devices with high stability. *Advanced Functional Materials* **2016**, *26* (32), 5903-5912.

(10) Dong, Y.; Gu, Y.; Zou, Y.; Song, J.; Xu, L.; Li, J.; Xue, J.; Li, X.; Zeng, H. Improving all-inorganic perovskite photodetectors by preferred orientation and plasmonic effect. *Small* **2016**, *12* (40), 5622-5632.

(11) Jarwal, D. K.; Jingar, N.; Kulhar, M.; Kumar, R.; Bera, A. Development of high-performance ultrafast photodetector using CsPbBr3 perovskite single crystal. *Sensors and Actuators A: Physical* **2024**, *374*, 115451.

(12) Jiang, N.; Wei, J.; Lv, M.; Rong, Y.; Wang, C.; Liu, Y.; Wei, G.; Han, X.; Wang, Y.; Liu, Y. Phase evolution and fluorescence stability of CsPb 2 Br 5 microwires and their application in stable and sensitive photodetectors. *Journal of Materials Chemistry C* **2023**, *11* (18), 6046-6056.

(13) Zhou, H.; Song, Z.; Grice, C. R.; Chen, C.; Zhang, J.; Zhu, Y.; Liu, R.; Wang, H.; Yan, Y. Self-powered CsPbBr3 nanowire photodetector with a vertical structure. *Nano Energy* **2018**, *53*, 880-886.

(14) Li, Y.; Shi, Z.-F.; Li, S.; Lei, L.-Z.; Ji, H.-F.; Wu, D.; Xu, T.-T.; Tian, Y.-T.; Li, X.-J. High-performance perovskite photodetectors based on solution-processed all-inorganic CsPbBr 3 thin films. *Journal of Materials Chemistry C* **2017**, *5* (33), 8355-8360.

(15) Suhail, A.; Saini, A.; Beniwal, S.; Bag, M. Tunable Optoelectronic Properties of CsPbBr3 Perovskite Nanocrystals for Photodetectors Applications. *The Journal of Physical Chemistry C* **2023**, *127* (34), 17298-17306.

(16) Zhou, H.; Zeng, J.; Song, Z.; Grice, C. R.; Chen, C.; Song, Z.; Zhao, D.; Wang, H.; Yan, Y. Self-powered all-inorganic perovskite microcrystal photodetectors with high detectivity. *The journal of physical chemistry letters* **2018**, *9* (8), 2043-2048.

(17) Bao, C.; Chen, Z.; Fang, Y.; Wei, H.; Deng, Y.; Xiao, X.; Li, L.; Huang, J. Low-noise and large-linear-dynamic-range photodetectors based on hybrid-perovskite thin-single-crystals. *Advanced materials* **2017**, *29* (39), 1703209.

(18) Sim, K. M.; Swarnkar, A.; Nag, A.; Chung, D. S. Phase Stabilized α-CsPbI3 Perovskite Nanocrystals for Photodiode Applications. *Laser & Photonics Reviews* **2018**, *12* (1), 1700209.

(19) Sun, Z.; Wang, Y.; Liu, Y.; Liu, R.; Chen, T.; Ye, S.; Lai, N.; Cui, H.; Lin, F.; Wang, R. Nanometer-Thick CsPbBr3 Films with Embedded CsPb2Br5 Nanowires for Photodetector Applications. *ACS Applied Nano Materials* **2024**.

(20) Tao, H.; Wang, H.; Bai, Y.; Zhao, H.; Fu, Q.; Ma, Z.; Long, H. Efficient photodiode-type photodetectors with perovskite thin films derived from an MAPbI 3 single-crystal precursor. *Journal of Materials Chemistry C* **2020**, *8* (18), 6228-6235.

(21) Ji, L.; Hsu, H.-Y.; Lee, J. C.; Bard, A. J.; Yu, E. T. High-performance photodetectors based on solution-processed epitaxial grown hybrid halide perovskites. *Nano letters* **2018**, *18* (2), 994-1000.

(22) Kim, H.-J.; Oh, H.; Kim, T.; Kim, D.; Park, M. Stretchable photodetectors based on electrospun polymer/perovskite composite nanofibers. *ACS Applied Nano Materials* **2022**, *5* (1), 1308-1316

(23) Lee, C.; Kim, K.; Shin, Y.; Han, D.; Yoon, S. J. In situ spectroelectrochemical investigation of perovskite quantum dots for tracking their transformation. *Frontiers in Energy Research* **2021**, *8*, 605976.